To Investigation the Structure and Morphology of Iron Metallic by Difference Techniques

Halo Dalshad Omar [*]

Department of Physics, School of Science, Faculty of Science and Health, University of Koya, Koya, Kurdistan Region, Iraq

Abstract: The characters of metal powder particles are depending on their size, shape and chemical surrounding. In sample preparation it is very important to control the particle size, particle shape and morphology.

X-Ray Diffraction (XRD) (Model: Panalytical Empyrean) study is most important tool used in powder materials science. A discussion about simple and low cost preparation of iron powder by (Mini Mill 2 Panalytical) and preparation of the sample was rotating at 15 min and in the case of grinding of samples at high speed 659 rpm.

The surface morphology of α-Fe metallic powder was determined with Scanning Tunneling Microscope (STM) (Model: NT-MDT Solver Nano.).

X-ray fluorescence analysis is a powerful analytical tool for the determination of almost all the elements present in a sample. The spectra obtained were analyzed using a X-ray fluorescence (XRF) (Model: Rigaku-NEX CG). From the spectra obtained, there were some elements to be present in the sample were Iron (Fe) and Zirconium (Zr).

Keywords: XRD, Structure of iron metallic, Crystallite Size, STM, Topography, XRF, XRF analysis.

1 Introduction

X-Ray Diffraction (XRD) used to determine peak position was carried out using a Panalytical. Operating at 45 kV and 40 mA, with a Cu X-ray tube ($\lambda = 0.15406$ nm) equipped with a 1x1 mm2 point focus and a Nickel filter on the direct beam path to absorb the Cu Kß radiation. The incident beam is collimated with a 1mm. Diameter collimator and focused on the sample mounted on a four-circle goniometer and the crystal structure of alpha iron is body centered cubic (BCC) [1-3].

The arrangement of atoms within the unit cell is associated with the relative intensities of these peaks. Intensities of diffracted beams are determined by positions of the atoms within the unit cell. STM images for surface morphologies of α-Fe are as shown in Fig.2.

X-ray fluorescence (XRF) is a very simple analytical technique; X-rays excite atoms in a sample, which emit X-rays at energies characteristic of each element. The process of detecting and analyzing the emitted x-rays is called " X-ray Fluorescence Analysis." In most cases the innermost K and L shells are involved in X-ray Fluorescence detection [3-7]. Structure and morphology its characterizations (XRD, STM and XRF) are studied in this research paper. A detector measures the energies and intensities of the emitted X-rays.

2 Iron Mettalic Powder Preparation

Before grinding iron metallic powder by Mini Mill 2 Panalytical was cleaned the bowl with acetone for a short time. The hardness of the grinding bowl used and of the grinding balls must be higher than of the Fe used. The grinding bowls and grinding balls of iron are resistance to acids with the exception of hydrofluoric acid.

In accordance with the application, the grinding time should be adapted of the bowl.

Iron metallic powders have investigated at 15 min and in the case of grinding of samples at high speed 659 rpm.

[*]Corresponding author e-mail: halo.dalshad@koyauniversity.org

3 X-Ray Diffraction Studies

X-ray diffraction is one of the most important characterization tools used in solid state chemistry and materials science [8]. XRD is an easy tool to determine the size and the shape of the unit cell for any compound. Powder Diffraction Methods is useful for Qualitative analysis: Phase Identification, Lattice parameter determination & etc. Diffraction pattern gives information on size and shape of the unit cell from Peak Positions and information on electron density inside the unit cell, namely where the atoms are located from Peak Intensities [12].
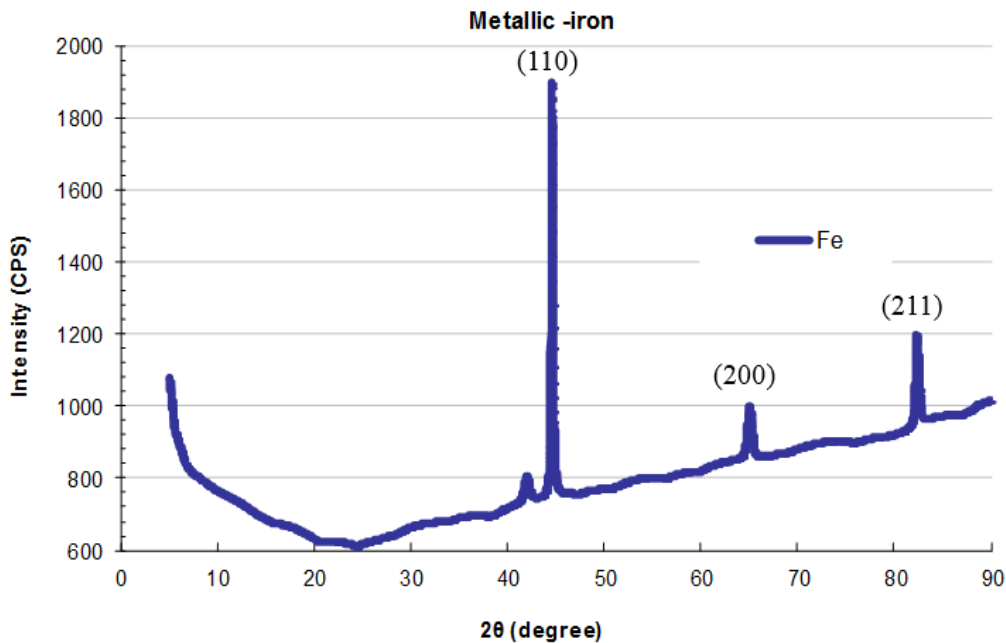

Figure.1. X-ray diffraction patterns of polycrystalline α-iron metallic powder.

Indexing is the process of determining the unit cell dimensions from the peak positions. It is the first step in diffraction pattern analysis. To index a powder diffraction pattern it is necessary to assign Miller Indices (h k l) to each peak.

XRD analysis of the prepared sample of iron metallic was done by a Panalytical (Under 45kV/40mA - X-Ray, 2θ/ θ-Scanning mode). Data was taken for the 2θ range of 5 to 90 degrees with a step of 0.013 degree. Data for some 2θ range has given in Table.1. Indexing process of powder diffraction pattern was done and Miller Indices (h k l) to each peak was assigned in first step [6]. Diffractogram of the entire data is in Fig.1.

3.1 Calculation of D-Spacing

The crystal structure of alpha iron is body centered cubic, with a unit cell edge a = 2.86 Å [5]. Following formulas a reused in the calculation of the expected 2θ positions of the first three peaks in the diffraction pattern and the interplanar spacing d for each peak [2].

$$\frac{1}{d^2} = \frac{h^2 + k^2 + l^2}{a^2}$$

(Eq. 1)

Bragg's Law is used to determine the 2θ value:

$$\lambda = 2d_{hkl} \sin \theta_{hkl}$$

(Eq. 2)

$$d = \frac{\lambda}{2.\sin \theta} (n = 1)$$

Wavelength λ = 1.5406(Å) for Cu $k\alpha 1$

1- $2\theta = 44.5859 \ (°)$ $\qquad d = \dfrac{1.5406(\overset{\circ}{A})}{2.\sin 22.29} = 2.0323(\overset{\circ}{A})$

2- $2\theta = 64.9805 \ (°)$ $\qquad d = \dfrac{1.5406(\overset{\circ}{A})}{2.\sin 32.490} = 1.43522(\overset{\circ}{A})$

3- $2\theta = 82.2971 \ (°)$ $\qquad d = \dfrac{1.5406(\overset{\circ}{A})}{2.\sin 41.148} = 1.17161(\overset{\circ}{A})$

The calculated d-spacing details are in Table. 1

3.2 Particle Size Calculation

From this study, considering the peak at degrees, average particle size has been estimated by using Debye-Scherrer formula [3-4-11].

$$D = \frac{0.9\lambda}{\beta \cos\theta} \qquad\qquad\qquad \text{(Eq. 3)}$$

Where 'λ' is wave length of X-Ray (1.5406(Å)), 'β' is FWHM (full width at half maximum), 'θ' is the diffraction angle and 'D' is particle diameter size.

1- $2\theta = 44.5859 \ (°)$ $\qquad \beta = 437.351 \times \dfrac{\pi}{180°} = 7.628(radians) \quad D = \dfrac{0.9 \times 1.540(\overset{\circ}{A})}{7.628 \times \cos 22.29} = 0.19(\overset{\circ}{A})$

2- $2\theta = 64.9805 \ (°)$ $\qquad \beta = 209.2548 \times \dfrac{\pi}{180°} = 3.650(radians) \quad D = \dfrac{0.9 \times 1.540(\overset{\circ}{A})}{3.650 \times \cos 32.490} = 0.450(\overset{\circ}{A})$

3- $2\theta = 82.2971 \ (°)$ $\qquad \beta = 398.7957 \times \dfrac{\pi}{180°} = 6.956(radians)$

$$D = \frac{0.9 \times 1.540(\overset{\circ}{A})}{6.956 \times \cos 41.148} = 0.264(\overset{\circ}{A})$$

Table.1 shows the experimentally obtained X-ray diffraction angle of α-Fe metallic powder. The XRD study confirms / indicates that the resultant particles are (BCC) iron powder.

Table. 1: Angular position, FWHM and grain size of the diffraction peaks for α-iron metallic (BCC)

2θ of the intense peak (°)	Intensity (CPS)	FWHM (°)	d - spacing (Å)	Crystallite Size (Å)	Miller Indices (h k l)
44.5859	904.58	437.351	2.0323	0.190	110
64.9805	106.91	209.2548	1.43522	0.450	200
82.2971	225.91	398.7957	1.17161	0.264	211

Three peaks at 2θ values of 44.585, 64.980, and 82.297 deg corresponding to (110), (200), and (211) planes of iron were observed and compared with the standard powder diffraction.

4 Scanning Tunneling Microscopic

The STM provides real space atomic resolution images through tunneling current between a tip (Pt-Ir) and an iron surface [9-10].

The surface morphology of iron metallic powder was studied by scanning tunneling microscopic as shown in the fig. (2 & 3).

The STM analyses the surface of solid objects, producing images of higher resolution. It produces representation of three dimensional sample from a diverse range of material. From STM images it was found that the root mean square roughness that the image 40 x 40 um scanning areas with 550 x 550 points, and scanning rate of 0.8 Hz, applied voltage 2.98 nV and the current between surface iron metallic and tip was 10.0 nA.
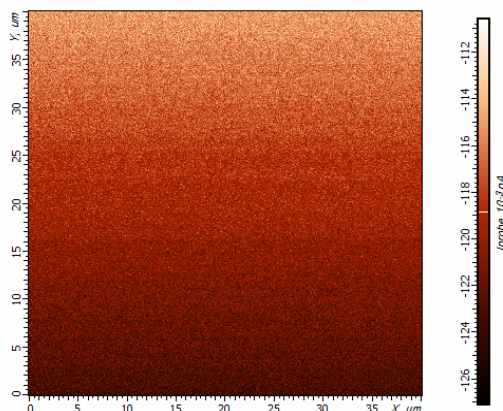

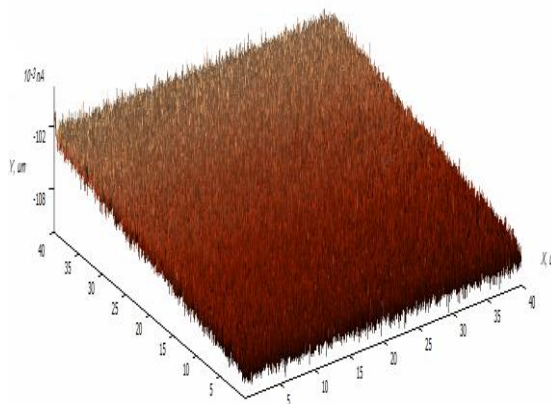**Figure.2.** Image 2D of iron metallic by STM-40 x 40 um

Figure.3. Image 3D of iron metallic by STM 40 x 40 um
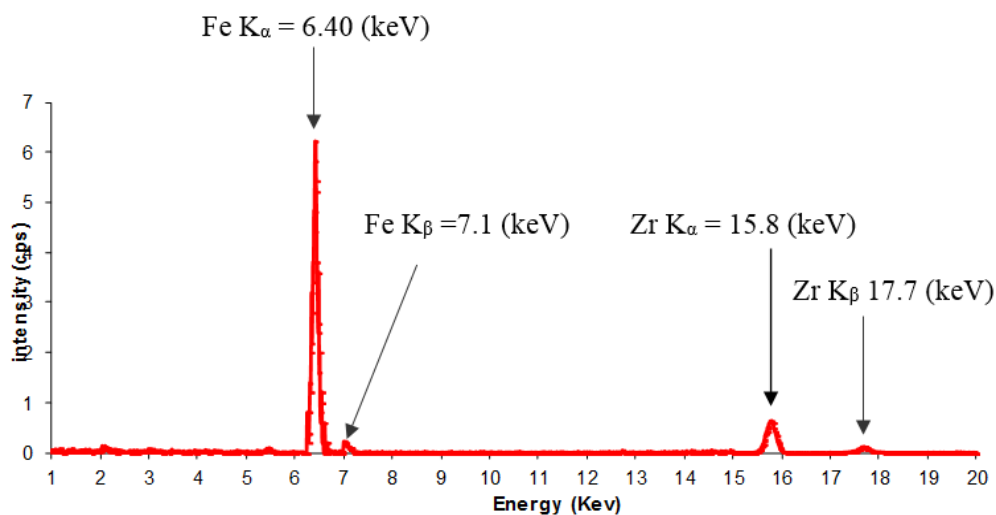
5 X-Ray Fluorescence

Figure.4. Shows the measured energy spectrum and identifies the major peaks (Fe, Zr)

The peaks in the spectrum correspond to the elements in the sample. The number of X-ray in each peak is proportional to the number of atoms. Finds the intensity of each peak, and computes the concentration of each element in the sample. Each element emits a unique spectrum of X-rays characteristic of that element. α-Fe has a strong peak at 6.40 keV and has a weak at 7.1 keV. The Zr peaks are very weak, indicating that there is Zr at 15.8 and 17.7 keV as shown in the figure 4. The tube voltage and tube current can be set within 25 kV and 1.0 mA respectively.

The measured intensity of single emission line depends on the energy spectrum and of exciting X-rays, on the efficiency of the detector and the geometry of source and sample. It also depends on the other elements in the sample.

6 Result and Conclusion

X-ray diffraction is an easy and one of the most important characterization tools used in powder materials research field. Three peaks at 2θ values of 44.585, 64.980, and 82.297 deg corresponding to (110), (200), and (211) of iron planes and body center cubic iron phase- standard powder diffraction card.

The XRD study confirms / indicates that the resultant particles are (BCC) alpha iron metallic powder by diffraction pattern presented in the Fig.1.

The surfaces of the products of α-Fe metallic were obviously smooth. The evaluated root mean square (RMS) surface roughness of the films was 2.07 nm for sample, as seen in the Fig. (2 & 3)

The XRF study confirms / indicates that the resultant of the alpha iron metallic powder by the spectrum obtained, there were a strong peak at 6.40 keV and has a weak at 7.1 keV as shown in the Fig.4.

Acknowledgements

References

[1] B. D. Cullity and S. R. Stock, Elements of X-Ray Diffraction, Associate Professor of Metallurgy in University of Notre Dame, 1978.

[2] Charles Kittel, Introduction to Solid State Physics (Wiley; 8th Edition, 2004)(ISBN 047141526X).

[3] Fairuz M. N, Bauk S. and Suzana M. I., XRF study on some Indian Mackerel samples, IJBAS-IJENS Vol: 12 No:03, June 2012.

[4]Viktor Hauk, Nin-destructive methods of measurement of residual stresses, Imtitut fiir, Rhei~zisch-Wesfilische Technische Hochschule Aachen, D-5100 Aachen, FRG, advances in surf. Treatments vol.3, 87120.

[5] A. Le Priol, E. Le Bourhis, P.-O. Renault, P. Muller, and H. Sik, Structure-stress-resistivity relationship in WTi alloy ultra-thin and thin films prepared by magnetron sputtering, J. Appl. Phys. 113, 213504 (2013); doi: 10.1063/1.4808240.

[6] B. Girault, "Study of size and structure effects on nanostructured W/Cu composites elasticity in thin layer," Ph.D. dissertation (University of Poitiers, 2008).

[7] Bradner D. Wheeler, analysis of limestones and dolomites by X-ray fluorescence, The Rigaku Journal, Rigaku/USA, 199 Rosewood Drive, Danvers, MA 01923, USA, Vol. 16/ number 1/ 1999.

[8] V. S. Vinila1, Reenu Jacob, Anusha Mony, Harikrishnan G. Nair1, Sheelakumari Issac, Sam Rajan, Anitha S. Nair4, Jayakumari Isac, XRD Studies on Nano Crystalline Ceramic Superconductor PbSrCaCuO at Different Treating Temperatures, Crystal Structure Theory and Applications, 2014, 3, 1-9.

[9] Alan Lawley, International Journal of Powder Metallurgy – Focus Issue: Precious Metals, Platinum Metals Rev., 2010, 54, (2), 122–124.

[10] T Machleidt, E Sparrer, D Kapusi and K-H Franke, Deconvolution of Kelvin probe force microscopy measurements—methodology and application, measurement science and technology, 20 (2009) 084017 (6pp).

[11] Nawal Kishore and S. Mukherjee, Synthesis and Characterization of Terbium (Tb) and Europium (Eu) Doped Mixed Ferrites, Journal of Nanotechnology & Advanced Materials An International Journal, 3, No. 1, 1-7 (2015).

[12] R. Saravanan, M. Prema Rani, Metal and Alloy Bonding - An Experimental Analysis: Charge Density in Metals and Alloys, springer, September 20, 2011.